



Original Article

Radion Effects on Dark Matter Fermions Production in e^+e^- Collisions

Truong Minh Anh^{1,*}, Ha Huy Bang², Pham Thi Diem²

¹*Faculty of Engineering Physics, Hanoi University of Science and Technology,
1 Dai Co Viet, Hanoi, Vietnam*

²*VNU Hanoi University of Science, 334 Nguyen Trai, Thanh Xuan, Hanoi, Vietnam*

Received 16th October 2024

Revised 12th November 2024; Accepted 22nd April 2025

Abstract: In this work, we investigate the effects of the radion on $e^+e^- \rightarrow \chi\bar{\chi}$ processes. The numerical results show that the cross-section with unparticle effects should be about 10^5 time larger than the one with photon effects. This could have important implications for dark matter searches.

Keywords: Radion, dark matter, cross section.

1. Introduction

As well known, astrophysical observations have shown that Dark Matter (DM) exists in our universe. In several extensions of the standard Model, dark matter fermions are postulated [1-5]. On the other hand, searching for the new physics effects, the e^+e^- linear colliders have an exceptional advantageous for its appealing clean background, and the possibility for the options of $e\gamma$ and $\gamma\gamma$ colliders based on it.

Remarkably, we have investigated unparticle effects on Bhabha scattering [6] and on axion-like particles production in e^+e^- collisions [7].

In this work, we extend the previous study [4] to obtain the production of dark matter fermion in the annihilation of the electron-positron pair via radion exchange.

2. The Cross Sections

We need to note that the radion-fermion-anti fermion vertex is corresponding to

* Corresponding author.

E-mail address: anh.truongminh@hust.edu.vn

<https://doi.org/10.25073/2588-1124/vnumap.4971>

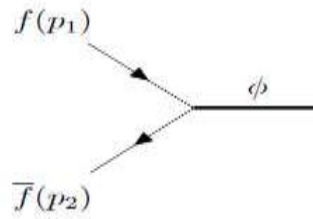


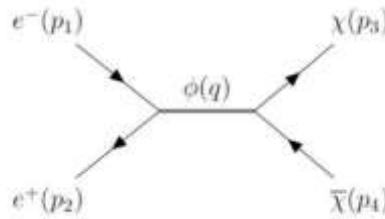
Figure 1. The radion-fermion-anti fermion vertex.

$$V_{\phi f\bar{f}} = \frac{-3i}{2\langle\phi\rangle} \left[\hat{p}_1 - \hat{p}_2 - \frac{8}{3}m_f \right], \quad (1)$$

The propagator of radion has the form

$$D_\phi = \frac{-i}{q^2 - m_\phi^2 + i\varepsilon}, \quad \text{Here } q \text{ is the 4 - momentum of radion.} \quad (2)$$

Now, let us investigate the effects of radion on $e^+(p_2)e^-(p_1) \rightarrow \chi(p_3)\bar{\chi}(p_4)$ process. This process is described by the Feynman diagram presented in Fig. 2.

Figure 2. Feynman diagram for $e^+e^- \rightarrow \chi\bar{\chi}$ process via radion.

The amplitude for this process is given by

$$M = \bar{v}(p_2) \frac{-3i}{2\langle\phi\rangle} \left[\hat{p}_1 - \hat{p}_2 - \frac{8}{3}m_e \right] u(p_1) \frac{-i}{q^2 - m_\phi^2 + i\varepsilon} \bar{u}_\chi(p_3) \frac{-3i}{2\langle\phi\rangle} \left[-\hat{p}_3 + \hat{p}_4 - \frac{8}{3}m_\chi \right] v_\chi(p_4), \quad (3)$$

So, the matrix element square is

$$|M|^2 = \frac{784m_e^2m_\chi^2}{(q^2 - m_\phi^2)^2 \cdot \langle\phi\rangle^2} \left[(p_2 p_1) - m_e^2 \right] \left[(p_3 p_4) - m_\chi^2 \right]. \quad (4)$$

In center of mass frame, four-momenta of particles are defined

$$\begin{aligned} p_1 &= (E, \vec{p}), p_2 = (E, -\vec{p}), \\ p_3 &= (E, \vec{k}), p_4 = (E, -\vec{k}), \\ q^2 &= (p_1 + p_2)^2 = 4E^2 = s. \end{aligned} \quad (5)$$

Therefore

$$p_1 p_2 = \frac{s}{2} - m_e^2, \quad p_3 p_4 = \frac{s}{2} - m_\chi^2,$$

$$|\vec{p}| = \frac{\sqrt{s}}{2} \sqrt{1 - \frac{4m_e^2}{s}}, |\vec{k}| = \frac{\sqrt{s}}{2} \sqrt{1 - \frac{4m_\chi^2}{s}}. \quad (6)$$

The differential cross-section can be obtained as follows

$$\frac{d\sigma}{d\Omega} = \frac{49}{36} \frac{m_e^2 m_\chi^2}{\pi^2 s \langle \phi \rangle^2} \frac{|\vec{k}|}{|\vec{p}|} \frac{1}{(q^2 - m_\phi^2)^2} [(p_2 p_1) - m_e^2] [(p_3 p_4) - m_\chi^2], \quad (7)$$

or

$$\frac{d\sigma}{d\Omega} = \frac{49}{144} \frac{m_e^2 m_\chi^2}{\pi^2 \langle \phi \rangle^2} \frac{\sqrt{1 - \frac{4m_\chi^2}{s}} (s - 2m_\chi^2)}{(s - m_\phi^2)^2}. \quad (8)$$

From (8), we get the total cross section is

$$\sigma = \frac{49}{36} \frac{m_e^2 m_\chi^2}{\pi \langle \phi \rangle^2} \frac{\sqrt{1 - \frac{4m_\chi^2}{s}} (s - 2m_\chi^2)}{(s - m_\phi^2)^2}. \quad (9)$$

3. Numerical Results and Discussions

Let us now turn to the numerical analysis. We take $m_\chi = 10 \text{ MeV} - 30 \text{ MeV}$, $m_e = 0.511 \text{ MeV}$, $m_\phi = 200 \text{ GeV}$, $\langle \phi \rangle = 1.0, 1.5, 1.7$ and 4.0 TeV as input parameters [8, 9].

Let us plot the σ respect to \sqrt{s} for $\langle \phi \rangle = 1.0, 1.5, 1.7 \text{ TeV}$ and for $m_\chi = 10 \text{ MeV}$ (Fig. 3), for $m_\chi = 20 \text{ MeV}$ (Fig. 4) and $m_\chi = 30 \text{ MeV}$ (Fig. 5). As can be seen,

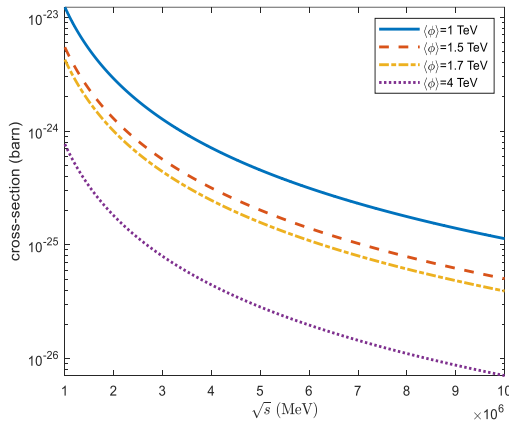


Figure 3. The variation of σ as a function of \sqrt{s} .

Here we take $m_\chi = 10 \text{ MeV}$.

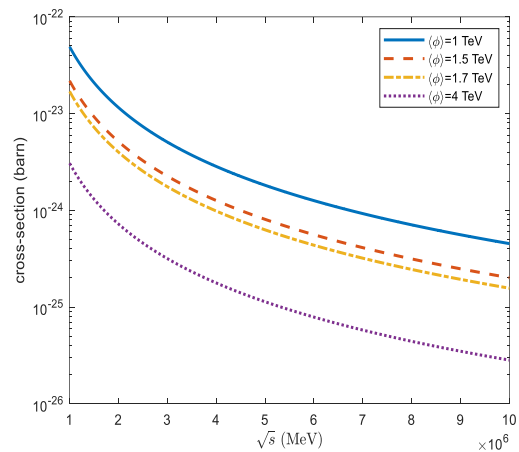


Figure 4. The total of cross-section is shown as a function of \sqrt{s} for $m_\chi = 20 \text{ MeV}$.

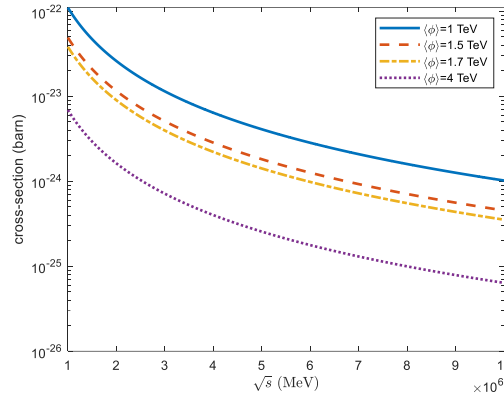


Figure 5. The total of cross-sections as a function of \sqrt{s} for $m_\chi = 30$ MeV.

The total cross section varies only little with the m_χ .

We give the numerical values of variation of total cross section as a function of m_χ for $\sqrt{s} = 1$ TeV and $\langle\phi\rangle = 1.0$ TeV - 4.0 TeV in Table 1.

Table 1. The variation of total cross section as a function of m_χ for $\sqrt{s} = 1$ TeV

m_χ (MeV)	σ (barn)			
	$\langle\phi\rangle = 1.0$ TeV	$\langle\phi\rangle = 1.5$ TeV	$\langle\phi\rangle = 1.7$ TeV	$\langle\phi\rangle = 4.0$ TeV
10	1.2277e-23	5.4565e-24	4.2481e-24	7.6732e-25
20	4.9109e-23	2.1826e-23	1.6993e-23	3.0693e-24
30	1.1049e-22	4.9109e-23	3.8233e-23	6.9059e-24

Next, we present the variation of σ as a function of \sqrt{s} for $m_\chi = 10$ MeV, 20 MeV, 30 MeV and for $\langle\phi\rangle = 1.0$ TeV (Fig. 6), for $\langle\phi\rangle = 4.0$ TeV (Fig. 7).

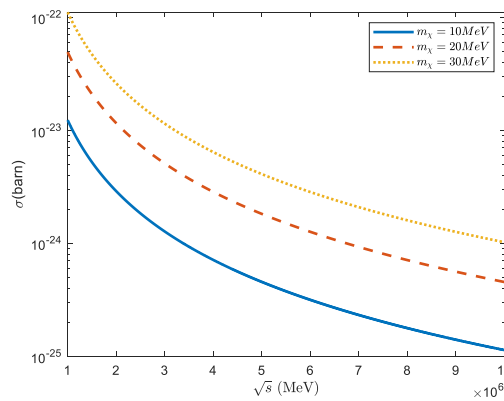


Figure 6. Total cross-section due to the radion contribution depending on the center of mass energy. Here, we assume $\langle\phi\rangle = 1.0$ TeV

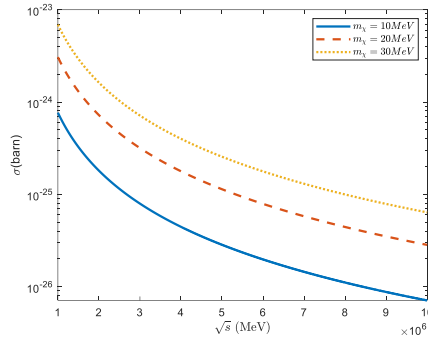


Figure 7. Dependence of the radion contributed total cross-section on \sqrt{s} . We assume $\langle\phi\rangle = 4.0$ TeV.

In the same way above mentioned, we have determined the differential and total cross-section for the process $e^+e^- \rightarrow \chi\bar{\chi}$ via exchange of photon.

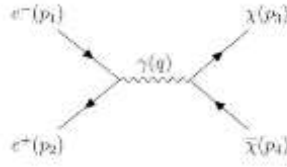


Figure 8. Feynman diagram for $e^+e^- \rightarrow \chi\bar{\chi}$ process through a photon.

In Ref. [4] the differential cross-section for process $e^+e^- \rightarrow \chi\bar{\chi}$ via photon is

$$\frac{d\sigma}{d\Omega} = \frac{\alpha}{16s\pi} \sqrt{1 - \frac{4m_\chi^2}{s}} \left\{ m_\chi^2 \left[s(1 - \cos^2 \theta) + 4m_\chi^2(1 + \cos^2 \theta) \right] + d_\chi^2(1 - \cos^2 \theta)(s - 4m_\chi^2) \right\}. \quad (10)$$

And total cross-section takes the form

$$\sigma_\gamma = \frac{\alpha}{6s} \sqrt{1 - \frac{4m_\chi^2}{s}} \left\{ m_\chi^2(s + 8m_\chi^2) + d_\chi^2(s - 4m_\chi^2) \right\}. \quad (11)$$

To compare the contributions, we give the ratio of the total cross-section with radion effects σ of (9) to the σ_γ of (14) as follows:

$$\frac{\sigma}{\sigma_\gamma} = \frac{49 \times 137}{6} \frac{m_e^2 m_\chi^2 [s - 4m_\chi^2] s}{\pi \langle\phi\rangle^2 (s - m_\phi^2)^2 \left[\mu_\chi^2 (s + 8m_\chi^2) + d_\chi^2 (s - 4m_\chi^2) \right]}.$$

From (12), we have obtained the ratio at different energies in Table 2.

Table 2. The ratio of total cross section with radion effects to one with photon effects

m_χ (MeV)	10	20	30
$\frac{\sigma}{\sigma_\gamma}$	5.4950e+04	2.1980e+05	4.9455e+05

Here we take $\mu_\chi = d_\chi = \frac{1}{3.3 \times 10^{12}}$, $m_\phi = 200$ GeV, $\sqrt{s} = 1$ TeV, $m_\chi = 10$ MeV; 20 MeV; 30 MeV, $m_e = 0.511$ MeV, $\langle \phi \rangle = 1$ TeV

The result above show that the total cross section of (9) is larger than the one in (12) by 5 orders of magnitudes. From this, we hope that there will be more ability to hunt Dark Matter fermions.

In summary, we have examined the radion effects at $e^+e^- \rightarrow \chi\bar{\chi}$. From numerical results, we have found that the effects of the radion on cross-sections can be strong. If the measurement is carried out at $\sqrt{s} = 100$ GeV – 1000 GeV, then the cross section for the process $e^+e^- \rightarrow \chi\bar{\chi}$ should be detectable. These could have important implications for the dark matter fermion and radion searches at future colliders. Our work can be extended for other scatterings, for example $e^+e^- \rightarrow \phi\phi$ process, here ϕ is the dark matter scalar. Works along these lines are in progress.

Acknowledgment

This research is funded by the Hanoi University of Science and Technology (HUST) under project number T2022-PC-057.

References

- [1] Y. Mambrini, T. Toma, X-ray Lines and Self-interacting Dark Matter, Vol. 75, No. 570, 2015, <https://link.springer.com/article/10.1140/epjc/s10052-015-3788-8> (accessed on: September 1st, 2024).
- [2] The CMS Collaboration, Search for Dark Matter and Unparticles in Events with a Z Boson and Missing Transverse Momentum in Proton-proton Collisions at $\sqrt{s} = 13$ TeV, Journal of High Energy Physics, Vol. 2017, No. 61, 2017, [https://link.springer.com/article/10.1007/JHEP03\(2017\)061](https://link.springer.com/article/10.1007/JHEP03(2017)061) (accessed on: September 1st, 2024).
- [3] R. Bartels, D. Gaggero, C. Weniger, Prospects for Indirect Dark Matter Searches with MeV Photons, Journal of Cosmology and Astroparticle Physics, Vol. 2017, 2017, <https://doi.org/10.48550/arXiv.1703.02546>.
- [4] A. Guha, J. Selvaganapathy, P. K. Das, Q-deformed Statistics and the Role of a Light Fermionic Dark Matter in the Supernova SN1987A Cooling, Phys. Rev. D, Vol. 95, Iss.1, 2017, pp. 015001, <https://doi.org/10.48550/arXiv.1509.05901>.
- [5] P. H. Gn, X.G. He, Electrophilic Dark Matter with Dark Photon: From DAMPE to Direct Detection, Phys. Lett. B, Vol. 778, 2018, pp. 292-295, <https://doi.org/10.1016/j.physletb.2018.01.057>.
- [6] S. T. L. Anh, T. Q. Trang, N. T. Huong, H. H. Bang, Unparticle Effects on Bhabha Scattering, Canadian Journal of Physics, Vol. 96, No. 3, 2018, pp. 268-271, <https://cdnsiencepub.com/doi/abs/10.1139/cjp-2016-0955> (accessed on: September 1st, 2024).
- [7] S. T. L. Anh, P. T. H. Trang, N. T. Trang, H. H. Bang, Unparticle Effects on Axion-Like Particles Production in e^+e^- Collisions, Vol. 57, 2018, pp. 2015-2021, <https://link.springer.com/article/10.1007/s10773-018-3727-1> (accessed on: September 1st, 2024).
- [8] arXiv: High Energy Physics – Phenomenology, Reconciling Small Radion Vacuum Expectation Values with Massive Gravitons in an Einstein-Gauss-Bonnet Warped Geometry Scenario, <https://arxiv.org/abs/1307.3018> (accessed on: September 1st, 2024).
- [9] U. Maitra, B. Mukhopadhyaya, S. SenGupta, Radion Vacuum Expectation Value and Graviton Mass: a Study in an Einstein–Gauss–Bonnet Warped Geometry Scenario, General Relativity and Gravitation, Vol. 48, No. 17, 2016, <https://link.springer.com/article/10.1007/s10714-015-2014-1> (accessed on: September 1st, 2024).